JOURNAL OF PROPULSION AND POWER
Vol. 24, No. 3, May–June 2008

Technical Notes

TECHNICAL NOTES are short manuscripts describing new developments or important results of a preliminary nature. These Notes should not exceed 2500 words (where a figure or table counts as 200 words). Following informal review by the Editors, they may be published within a few months of the date of receipt. Style requirements are the same as for regular contributions (see inside back cover).

Infrared Signature Suppression of Helicopter Engine Duct Based on "Conceal and Camouflage"

S. P. Mahulikar,* H. S. S. Prasad,† and S. K. Potnuru‡
Indian Institute of Technology, Bombay, Mumbai 400076, India

DOI: 10.2514/1.28636

Nomenclature

Bi	=	Biot number
D	=	diameter, m
E	=	hemispherical emissive power in rear view, W
e	=	hemispherical emissive flux in rear view, W/m^2
H	=	helicopter altitude, km
k	=	thermal conductivity, W/m · K
L	=	length, m
$\dot{m}_e$	=	mass flow rate through engine, kg/s
P_H	=	helicopter susceptibility
T	=	temperature, K/°C
t	=	thickness, m
α	=	semicone angle of module 2, deg /rad
ε	=	surface emissivity
λ	=	wavelength, μm
$\xi_{\min}$	=	minimum signal-to-noise ratio required for lock-on
ρ	=	density, kg/m^3
ϕ	=	view angle, deg /rad
Ω	=	solid angle, sr

Subscripts

conf1, conf2	=	configurations 1, 2, respectively
crit	=	critical value based on material constraint
ed	=	exhaust duct
ex	=	exit
g	=	gases in engine exhaust duct
gw	=	glass wool
i	=	inner surface (for module 1)/interfacial surface (for module 2)
in	=	inlet
max	=	maximum value
o	=	outer surface
w	=	wall
$\lambda1$–$\lambda2$	=	in wavelength band $\lambda1$–$\lambda2$
1, 2	=	modules 1, 2, respectively
∞	=	ambient parameter
*	=	selected value of design parameter for IRSS system

Received 1 November 2006; revision received 17 June 2007; accepted for publication 28 November 2007.

*Associate Professor and A. von Humboldt Fellow, Department of Aerospace Engineering; spm@aero.iitb.ac.in.

†Masters' Student, Department of Aerospace Engineering; Permanent Affiliation: Chief Manager, Rotary Wing Research and Design Centre, Hindustan Aeronautics Ltd., Bangalore, India.

‡Masters' Student, Department of Aerospace Engineering.

Introduction

STEALTH techniques have an impact on the design of aerospace vehicles that must operate in a human-made hostile environment [1,2]. The passive nature of infrared (IR) detectors makes them suitable for acquiring a target at sufficient ranges and for providing sufficient engagement boundaries [2,3]. Atmospheric attenuation of IR radiation is low in 1–2.5 μm, 3–5 μm, and 8–12 μm bands. Therefore, they are called *atmospheric windows* [2,4] and are used for detection, tracking, and lock-on. Developments in IR detection and tracking led to the increasing effectiveness of IR-guided missiles [2,5]. About 89% of downed aircraft and helicopters between 1979 and 1993 were due to IR-guided surface-to-air missiles (SAMs) and air-to-air missiles [2,6,7].

Background and Motivation

The air defense systems comprising IR-guided threats are of even greater concern to the survivability of helicopters engaged for a tactical role [2,8]. Most IR-guided SAMs, including man portable air defense systems (MANPADS) have a burn-out range of 3–6 km [2,9], which is the normal operating altitude of helicopters. The fourth generation IR detectors use multispectral thermal imaging systems, which can detect an IR signature in a wide spectrum and can lock on to the helicopter from all aspects. More important, these systems are immune to IR countermeasures such as flares that appear as a point source and are discarded by the detector [2,10].

The difference in IR radiance levels between the helicopter and the background that it replaces can lead to detection followed by lock-on by an IR-guided missile [2,11]. The IR bands used for IR guidance are 1) 1.9–2.9 μm (used in first generation IR seekers), 2) 3–5 and 8–12 μm (current generation), and 3) multicolor that detects in two or three discrete IR wavelengths in the above three bands [2,12]. In the 8–12 μm band, the contrast of the helicopter frame against the background is sufficient to provide a detectable target. In the visible and 3–5 μm bands, reflected sunlight can play a significant role in providing a detectable target. Nevertheless, several IR-signature suppression (IRSS) systems focus on cooling the hot power plant parts, which are the dominant and reliable sources of the IR signature for both day- and night-time missions.

A suitable IRSS system can drastically reduce the IR-signature levels, by modifying radiance to match with the background [2,13]. The sources of the IR signature in a helicopter include the following: 1) engine exhaust duct, 2) exposed hot engine parts (e.g., power turbine blades), 3) exhaust plume heated tail boom, and 4) plume [2,7,8]. Sully et al. [7] presented the planar variation of the IR signature with viewing aspect for a helicopter in the 3–5 μm band, in which the power turbine blades are blocked by the exhaust duct. The plume heated section of the tail boom accounts for a significant amount of IR signature from side-on to rear view angles. However, the plume IR signature is only 10% of the signature of the exhaust

metal duct from rear view angles. Thompson et al. [8] presented the IR-signature breakdown of the Bell-205 (UH-1H) helicopter in the 3–5 μm band. It was shown that the engine exhaust plume is the least contributor, followed by the tail boom heated by the plume. Unlike metals, the exhaust plume exhibits band emissivity and emits selectively in discrete bands [2,14]. There is no emission from the plume in the 8–12 μm band; however, surfaces of solids being gray, they emit at all wavelengths at all temperatures. Therefore, the direct view of the power turbine stages at 600–700°C and the tail pipe are the most dominant contributors. For upturned exhausts, the plume IR-signature contribution is further suppressed due to the accelerated mixing with the ambient air by the downwash of the main rotor.

The important expectations from an IRSS system are as follows: a) the IR signature from the exposed surfaces must be well within acceptable limits, over the operating regime that is prone to threat from IR-guided missiles; 2) visibility of hot surfaces that cannot be completely blocked must be restricted to a narrow range of viewing aspect angles; 3) engine power loss due to backpressure and the operation of the IRSS system, and weight and drag of the IRSS system, must be minimal; 4) available hard points on the helicopter should be harnessed for installation of the IRSS system as retrofit, with only minor modifications.

Cascaded Ejector-Based IRSS Systems

There are different types of IRSS systems for helicopter engines, designed depending on the requirements; prominent among them are the retrofits, the film-cooled tailpipe (FCT) and the center body tailpipe (CBT). The FCT IRSS system is a passive cascaded ejector, which was developed considering the following three important requirements: 1) SAMs as the main threat to helicopter operation, 2) minimal modification requirements to the helicopter for its installation, and 3) less engine backpressure penalty, because disturbance to exhaust flow is reasonably low. The FCT entrains secondary air by ejector action for film cooling of the tailpipe and plume cooling [7]. It is moderately effective in suppressing the IR signature from both visible metal and plume, for all flight conditions. A reduction in the IR signature of about 50% is achieved in the side view and about 20% in the rear view.

The CBT is a cascaded ejector, comprising a film-cooled outer duct surrounding a film-cooled center body, followed by a diffuser. In addition to the ejector (secondary) air cooling of the center body and plume, CBT has an optical block that prevents a direct view of the engine hot parts. The effectiveness of CBT as an IRSS system was tested on a Bell-205 (UH-1H) helicopter, and 80% reduction in the IR signature was observed from all viewing aspects. The major drawback of CBT (in addition to its higher weight than FCT) is the increased backpressure on the engine due to the presence of the center body and due to plume cooling. This backpressure results in about 3% power loss, for the engine operating point corresponding to 940 shp. Further, this optical block is heated, and for reducing its IR signature, there is an active fan-assisted CBT version, which cools the centerbody using ambient air. This active version extracts power from the main engine for its functioning and further reduces the power available for the mission.

Black Hole Ocarina IRSS System

The black hole ocarina (BHO) system used on the YAH-64 Apache helicopter is a low cost IR suppressor, without any moving parts such as a blower (unlike the fan-assisted CBT). It is a merger of black hole and ocarina systems, and has the advantages of a bent nozzle of the black hole system and multiple outlets of the ocarina system. However, the sharp bending of the nozzle introduces more losses and leads to impingement of high temperature exhaust gases on the bent, thereby creating hot spots.

Motivation for Development of Another IRSS System

The penalties introduced by the installation of the IRSS system essentially reduce the gain of IR suppression. As an illustration, the weight added due to installation of the IRSS system as a permanent feature needs additional power to perform the mission and restricts the maximum payload. The penalties can be interpreted in the following two perspectives: 1) for the same gas generator speed and fuel flow, the IRSS system reduces the power; 2) for the same power available for the mission, the IRSS system results in higher fuel flow, higher gas generator speed, and higher exhaust gas temperatures. In case 2, the engine operating point shifts, which increases the temperature of the IRSS system, thereby reducing its IR-suppression performance.

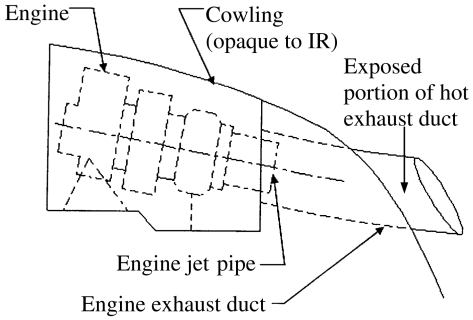

Fig. 1 Layout of typical semi-exposed engine installation on helicopter.

The IRSS-system design also depends on whether the engine installation is of a submerged, semi-exposed, or fully exposed type. Several current generation helicopters have gas turbine engines submerged inside the cowling (Fig. 1). The exhaust gases are redirected through a bent duct to prevent impingement on the helicopter structure, thereby optically blocking the hot engine parts (similar to the black hole system). Therefore, the important visible hot portion is the metallic exhaust duct that protrudes outside of the cowling.

Theoretical Concept of IRSS System Based on "Conceal and Camouflage"

A typical helicopter of the 4–5 ton class with two semi-exposed turboshaft engines of approximately 1000 shp is considered for the conceptual design of the IRSS system. Because the engine cowling is opaque to IR radiation, the IRSS system is conceptualized for the exposed portion of the metallic exhaust duct. The technique of stealth is to *conceal* the source of the IR signature, and to *camouflage* the exposed concealment with the background radiation that is replaced by the helicopter. As seen from below, the background radiation is the sky, which includes the atmosphere [15] and clouds at low altitudes. Therefore, the objective of the proposed IRSS system (Fig. 2) is to minimize the visibility of the hot metallic duct and to reduce the temperature of the outer surface of the IRSS system.

It is to be concurrently ensured that all the penalties associated with its installation are minimal; in particular, the engine exhaust flow is not disturbed. Restriction and/or diversion of the engine exhaust flow and the cooling of exhaust gases in the flow path (which increases their density, ρ) increase the engine backpressure penalty. The proposed IRSS system does not disturb the engine exhaust flow as in the case of FCT [7], which is known for its small engine backpressure penalty as compared to CBT. Unlike other IR suppressors, the entrained air and plume cooling are marginal; therefore, the hot gases can impinge and heat surfaces (e.g., main rotor blades). The plume heated surfaces can be separately treated by the emissivity optimization technique, which is elaborated on by Mahulikar et al. [16] for an aircraft engine. The IRSS system reduces heat transfer from the exhaust duct to the ambient; hence, the temperature of exhaust gases with the IRSS system installed is higher (for the same operating point). This has the effect of relieving the engine backpressure penalty, due to the lowering of ρ of the exhaust gases.

Significant turbulence arises from the ambient airstream flow over the helicopter body, because the flow pattern is not symmetrical (due to main rotor downwash). Therefore, the drag due to the protruding

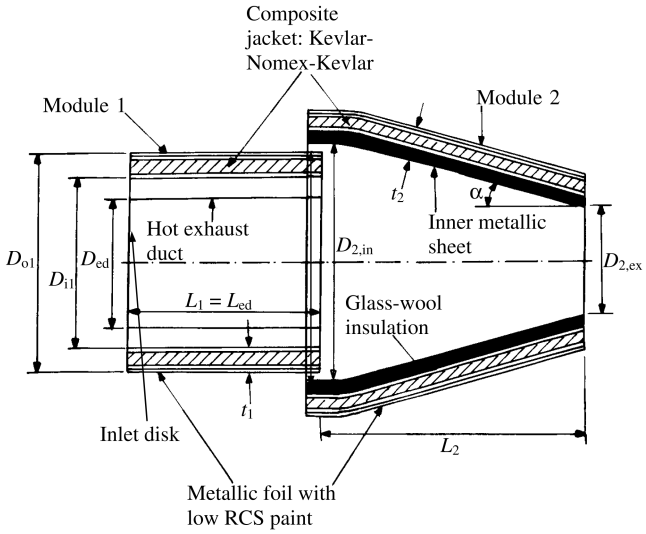

Fig. 2 Concept of the IRSS system for the helicopter engine exhaust duct.

engine exhaust duct is an insignificant percentage of the total helicopter drag. Though additional drag relative to the fully exposed engine exhaust duct is 40%, this increase relative to the helicopter drag is still insignificant.

Ease of manufacture and installation are also considered in the conceptual design of the IRSS system. Module 1 of the IRSS system is located over the engine exhaust duct by suitably designed joints spread over the circumference that also serve as stiffeners. Module 2 is located over module 1 also by similar stiffeners over the outer circumference of module 1 close to its exit. The moderate thermal conductivity of these stiffeners and their nominal thickness results in high thermal resistance. Therefore, the thermal design of the IRSS system is not degraded by fitments for its mounting for structural stability and integrity.

The visibility of the outer surface of the exhaust duct is completely blocked by the IRSS system, and the visibility of the inner surface is restricted to a narrow range of ϕ. The dynamic nature of tactical warfare continuously changes ϕ between the IR-guided missile and the target helicopter. An IR-guided missile cannot achieve sustained lock-on, if its IR detector does not receive a relatively steady IR-signature level that exceeds $\xi_{\min} \cdot \text{NEI}$ (noise equivalent irradiance). Therefore, restricting the visibility of hot parts to a narrow range of ϕ has an insignificant increment on P_H of a helicopter against IR-guided missiles. Figure 2 illustrates the concept of the IRSS system, designed to suppress the IR signature of the hot metallic duct of length L_{ed} and diameter D_{ed}; it consists of two modules (1 and 2). This metallic duct has a thickness slightly less than 1 mm, and being a good heat conductor, has $Bi < 0.1$; therefore, its inner and outer surface temperatures are the same. Both modules include a lightweight composite, which comprises Kevlar layers sandwiching a Nomex core. The stagnant air pockets in the Nomex core further improve the insulation, by lowering the effective k below that of the material. The inner/interfacial surface temperatures of modules 1, 2, respectively, are determined by the material constraint. The thickness of the modules is based on the highest acceptable temperature on their outer surfaces, which is based on the camouflage requirement. For given outer and inner/interfacial surface temperatures, lower k material reduces the thickness, which for given material ρ, reduces the weight. Because the composite is radar transparent, it is covered by a metallic foil with low radar cross-section (RCS) paint, in both the modules. This metallic jacket prevents the multiple internal reflections between the composite and inner metal surfaces (termed the "cavity effect"), which significantly increase RCS. The simplicity of the IRSS concept is expected to enhance its reliability, considering the requirement of a long lifetime functionality in a tough thermal and vibrational environment.

Concept of Module 1

Module 1 is a low ρ and low k cylindrical jacket of inner diameter D_{i1} ($>D_{ed}$), outer diameter D_{o1}, and length $L_1 = L_{ed}$. It optically blocks the outer surface of the exhaust duct from almost all ϕ, except for a very narrow range of ϕ that is completely blocked by module 2. The D_{i1} is determined based on the maximum temperature on the inner surface of module 1, which the material can withstand. The low k_1 also enables weight reduction by reducing t_1 for fixed temperatures on the outer and inner surfaces. Some ambient air is entrained through the annular space between the exhaust duct and module 1. This small airflow nominally cools the outer surface of the exhaust duct and the inner surface of module 1.

Concept of Module 2

Module 2 is a frustum of inlet and exit diameters, $D_{2,in}$ and $D_{2,ex}$, respectively, and length L_2, where $D_{2,in}$ slightly exceeds D_{o1}. Because the prime objective is concealment (and not cooling) of hot parts, specific efforts are not made to enhance heat removal by entrainment of secondary airflow. Optical blocking of hot parts is more effective in IR suppression than cooling by entraining more ambient air; hence, $D_{2,ex} \approx D_{ed}$. The $D_{2,ex}$ marginally exceeds D_{ed}, so that IR suppression by the optical blocking effect dominates cooling due to the entrainment of ambient air. Module 2 as a frustum with a semicone angle $\{=\tan^{-1}[(D_{2,in} - D_{2,ex})/(2L_2)]\}$ is more effective in optical blocking than an extension of cylindrical module 1 by length L_2. Unlike in module 1, the hot exhaust gases are in direct contact with the inner surface of module 2; hence, its inner surface has a thin metallic layer followed by glass-wool insulation. This glass-wool insulation is then covered by the same layout as in module 1, that is, a Kevlar–Nomex–Kevlar composite followed by a metallic foil with low RCS paint. Module 2 completely blocks the visibility of the outer surface of the hot exhaust duct and restricts the visibility of the inner surfaces of the exhaust duct and module 1.

Thermal Design of IRSS System

At the design point (DP), typical high values of $\dot{m}_e$(=2.4 kg/s) and T_g(=570°C) are considered, so that IRSS-system temperatures are conservatively estimated. At the DP, $T_\infty = -1$°C, and the temperatures on the inner and outer surfaces of the IRSS system are predicted by a multimode thermal analysis. The conjugate analysis comprises the convective heat transfer, surface radiation interchange, and radial conduction through the thickness. Because the thicknesses and k values of the modules are small, axial conduction through the modules is neglected. The mixing of the hot core and entrained annular streams at the exit plane is assumed to be adiabatic and instantaneous. The parameters after mixing are obtained by solving continuity, enthalpy balance, and momentum equations, simultaneously with the heat transfer equations. The radiance–irradiance approach is used for modeling the multiple reflections and scattering of radiation in the layout comprising the exhaust duct and the IRSS system. The multimode thermal analysis is a numerical procedure in which the layout is axially discretized (because circumferential variations in the parameters are insignificant). The governing conservation equations for each discretized element are arrived at from first principles, and solved for each element under steady state. The convective, conductive, and radiative heat fluxes at each surface of the discretized layout are also obtained from their respective definitions. The procedural details of the multimode thermal modeling are the same as reported by Mahulikar et al. [17,18] The thermal model is validated based on insignificant energy-balance error between the inlet and exit of the IRSS system. Using this model, the IRSS system is designed based on the following two thermal considerations:

1) the maximum allowable exposed surface temperature contrast $(T_{wo} - T_\infty)_{\max} = 25$°C, which is based on an IR-suppression performance requirement;

2) the maximum allowable temperature on the inner/interfacial surfaces of modules 1 and 2, $T_{wi,\max}$(=150°C), which is based on the material constraint.

Design of Module 1

Increases in $\varepsilon_{\mathrm{ed},o}$ and ε_{i1} during operation, for example, due to oxidation and surface wear, are uncertain. Therefore, for a conservative thermal design, it is necessary to select $\varepsilon_{\mathrm{ed},o}$ and ε_{i1} that would give high values of T_{wi1} and T_{wo1}. Higher $\varepsilon_{\mathrm{ed},o}$ increases emission from the outer surface of the hot exhaust duct, and higher ε_{i1} increases the absorption of incident irradiance on the inner surface of module 1. Both these effects increase the temperature of module 1; therefore, a high value of $\varepsilon_{\mathrm{ed},o}$ ($=\varepsilon_{i1} = 0.9$) is chosen for the design. The $\varepsilon_{\mathrm{ed},i}$ and ε_{o1} values are selected for the combination of material and expected surface characteristics.

The design parameter which most significantly affects the contrast temperature ($T_{wo1} - T_\infty$) is D_{i1}; for given H, ($T_{wo1} - T_\infty$) decreases with an increase in D_{i1}. This effect is due to the reduction in radiation heat transfer to module 1 from the hot exhaust duct. The ($T_{wo1} - T_\infty$) increases with an increase in H for given D_{i1}, mainly because of the decrease in T_∞ with increase in H. The IRSS performance requirement is met for $D_{i1} \geq D_{i1,\mathrm{DP}}$ and for selecting D_{i1} ($=D_{i1,^*} > D_{i1,\mathrm{DP}}$), maximum permissible $T_{wi1,\max}$ is estimated for the most severe operating condition. The variation of T_{wi1} with $T_{\infty,\mathrm{SL}}$ at different H for $D_{i1} = D_{i1,\mathrm{DP}}$ indicates that T_{wi1} increases with $T_{\infty,\mathrm{SL}}$ for given H and is highest at sea level (SL). Because the helicopter can operate at $T_{\infty,\max} = 55°\mathrm{C}$ (which is possible in an extreme desert summer condition), ISA + 40°C (ISA: international standard atmosphere) at a SL operating condition is considered for fixing D_{i1}. The T_{wi1} decreases approximately linearly with D_{i1}; and at $D_{i1} = D_{i1,^*}$, $T_{wi1} = 150°\mathrm{C}$, which is the temperature up to which the material is certainly not damaged. Therefore, selecting $D_{i1} = D_{i1,^*}$ ensures that the material temperature of module 1 is well within the acceptable limit for all operating conditions.

The performance of the designed module 1 is simulated using the multimode thermal model at ISA + 10°C and $H = 2$–4 km. The variation of the contrast temperature ($=T_{wo1} - T_\infty$) along the length is an inverted "U" shaped distribution, due to higher heat loss at the ends. The IR-suppression performance is best at lower H and gives an acceptable performance at DP. This performance characteristic is desirable, because low-flying helicopters are most prone to threats posed by IR-guided SAMs that are launched from the ground.

Design of Module 2

In module 2, the most critical temperature is that of the interface between glass wool and the composite, where the composite material has the highest temperature. The t_{gw} is chosen to reduce this interfacial temperature and also the maximum contrast temperature of the exposed surface of module 2 ($T_{wo2,\max} - T_\infty$). Figure 3 gives the variation at DP of $T_{wi2,\max}$ (interfacial temperature), $T_{wo2,\max}$ (outer surface temperature), and the contrast temperature ($T_{wo2,\max} - T_\infty$), with t_{gw}. For $t_{\mathrm{gw}} \geq t_{\mathrm{gw,crit}}$, $T_{wo2,\max} \leq 150°\mathrm{C}$ (based on material constraint), and for $t_{\mathrm{gw}} \geq t_{\mathrm{gw}^*}$, ($T_{wo2,\max} - T_\infty$) $\leq$ 25°C (based on performance constraint). Because $t_{\mathrm{gw}^*} > t_{\mathrm{gw,crit}}$, the selection of $t_{\mathrm{gw}} = t_{\mathrm{gw}^*}$ ensures that the material and contrast temperatures are acceptable over the operating range. Even for ISA + 40°C at SL, $T_{wo2,\max} < 150°\mathrm{C}$, thereby ensuring that the composite material temperature limit is never exceeded for $t_{\mathrm{gw}} = t_{\mathrm{gw}^*}$.

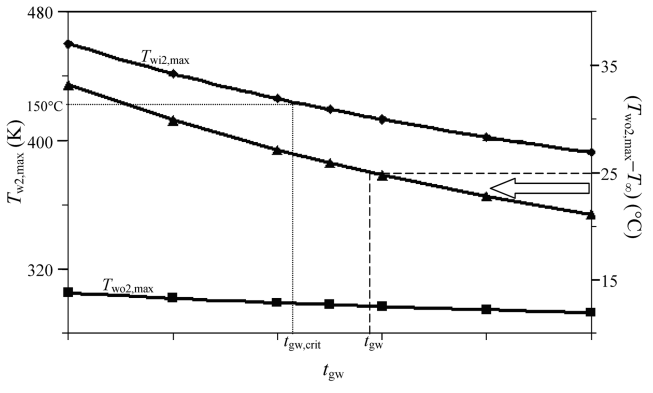

Fig. 3 Variation of module 2 temperatures with t_{gw}.

The length L_2 of module 2 is optimized, considering the diminishing returns of the gains due to P_H reduction, and the increasing penalties (weight and drag) with increasing L_2. The variation of rms hemispherical emissive power (E_{rms}) of the IRSS system from the rear view, with increasing L_2, is analyzed. The E_{rms} for the two IR bands of interest is given as

$$E_{\mathrm{rms}} = [(E_{3\text{–}5\ \mu\mathrm{m}})^2 + (E_{8\text{–}12\ \mu\mathrm{m}})^2]^{1/2}$$

where

$$E_{\lambda 1-\lambda 2} = \int_S e_{\lambda 1-\lambda 2} \cdot \cos\psi \cdot \mathrm{d}S$$

The $\cos\psi$ term projects the 3-D surface area (S) on a 2-D plane perpendicular to the axis of the IRSS system. As per Planck's law [19],

$$e_{\lambda 1-\lambda 2} = \int_{\lambda_1}^{\lambda_2} \frac{2\pi h \cdot c^2 \cdot \mathrm{d}\lambda}{\lambda^5 \cdot [\exp(\frac{c \cdot h}{\lambda \cdot k' \cdot T}) - 1]}$$

where c is the velocity of light in vacuum, h is Planck's constant, and k' is Boltzmann's constant. Figure 4 shows the variation of E_{rms} with L_2, which shows a monotonic decrease in the IR signature with an increase in L_2, but also a tendency toward diminishing returns. The L_{2^*} in Fig. 4 is determined based on the estimation of the lethal envelope [20], which is a measure of P_H of the helicopter. The P_H analysis was performed for $H = 4$ km, considering typical values of helicopter and missile velocities, and typical IR-detector characteristics (NEI and $\xi_{\min}$). The variation of P_H with L_2 is estimated in 3–5 μm and 8–12 μm bands, and it is found that P_H monotonically reduces with an increase in L_2. The variation of $[-(\mathrm{d}P_H/\mathrm{d}L_2)/P_H]$ with L_2 shows that the rate of change P_H goes through a maxima at an optimum $L_2(=L_{2^*})$; this optimum L_2 is higher for the 8–12 μm band. The variation of contrast temperature ($T_{wo2} - T_\infty$), at ISA + 10°C of the designed module 2 shows acceptable performance at DP and reasonable performance at higher H.

Optical Blocking of Exhaust Duct by IRSS System

The IR signature as perceived by a heat-seeking missile's IR detector is largely influenced by the operating temperature of the target and also the viewing aspect angle. To reduce P_H, the IRSS system minimizes the visibility of the hot surfaces, which include the inlet disk (Fig. 2), and the inner and outer surfaces of the exhaust duct. To estimate the effectiveness of optical blocking over a wide range of ϕ, Ω subtended by the hot surfaces of the layout is estimated by the *parallel rays projection* method [21]. Mahulikar et al. [21] developed this procedure using geometric optics for estimating the visibility of the internal and external hot parts of an aircraft engine. In this investigation, a similar procedure is developed for estimating Ω subtended by the surfaces of the layout comprising the hot engine exhaust duct and the IRSS system. For estimating the effectiveness of optical blocking by the IRSS system, Ω subtended by the visible surfaces of the exhaust duct are compared in the following two configurations: 1) configuration 1 (conf1): without the IRSS system installed, that is, only the hot exhaust duct is present; 2) configuration 2 (conf2): the IRSS system is mounted over the

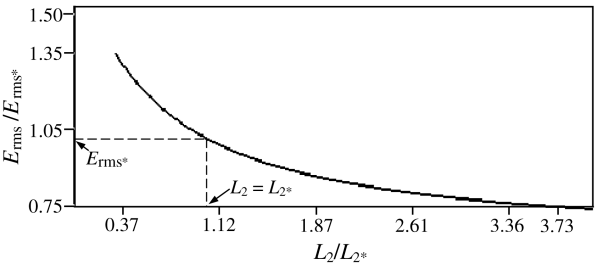

Fig. 4 Variation of E_{rms} with L_2.

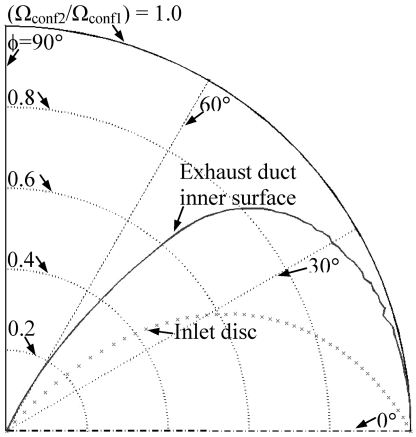

Fig. 5 Effectiveness of optical blocking of visible exhaust-duct surfaces.

hot exhaust duct. The Ω subtended by the surfaces in configurations 1 and 2 is obtained for ϕ varying from 0 deg (direct view from the rear) to 90 deg (view perpendicular to the exhaust-duct axis). The Ω subtended in the other half (ϕ varying from 90 to 180 deg) is its mirror image, due to symmetry. These variations are valid for any plane passing through the exhaust-duct axis, due to axisymmetry.

The three visible surfaces in configuration 1 are the inlet disk, and the inner and outer surfaces of the hot exhaust duct. The Ω subtended by the inlet disk is maximum at 0 deg, and decreases as ϕ increases and becomes zero before ϕ reaches 90 deg, at which point, the inlet disk is optically blocked. The Ω subtended by the inner surface of the exhaust duct first increases from zero, reaches a maxima, and then decreases to zero at 90 deg. The Ω subtended by the outer surface of the exhaust duct is zero at $\phi = 0$ deg, increases with ϕ, and is maximum at $\phi = 90$ deg.

In configuration 2, though the largest Ω subtended is by the outer surface of the IRSS system, it is not of concern, because it is camouflaged with the background by the thermal design. The visibility of the following surfaces is completely blocked (i.e., Ω subtended is zero) in configuration 2 for all ϕ: 1) the outer surface of the hot exhaust duct (because $D_{2,ex} \approx D_{ed}$), 2) the inner surface of module 1 of the IRSS system, 3) the annular disk on the helicopter cowling between the exhaust duct and module 1. Figure 5 compares Ω subtended by the inlet disk and the exhaust-duct inner surface, with and without the IRSS system, by plotting $(\Omega_{conf2}/\Omega_{conf1})$ versus ϕ. Module 1 provides significant optical blockage only to the exhaust-duct outer surface, but does not optically block the inner surface of the exhaust duct and the inlet disk (for any ϕ). Installation of modules 1 and 2 reduces the visibility of the exhaust-duct inner surface and the inlet disk, to a narrow range of ϕ. The limited visibility of the additional inner surface of module 2 in a restricted range of ϕ does not adversely affect P_H, due to the continuously changing ϕ in tactical warfare.

Conclusions and Summary

1) An infrared signature suppression system is conceptualized for a helicopter engine exhaust duct, based on *low observables* principles of conceal and camouflage.

2) The exposed surfaces of the IRSS system are camouflaged with the background by thermal design, which considers multimode heat transfer, including surface radiation interchange.

3) The IRSS system completely blocks the visibility of the exhaust-duct outer surface and the inner surface of its module 1. It reduces the solid angle subtended by the inlet disk surface and the inner surface of the hot exhaust duct, and also the range of the viewing aspect angle (ϕ) over which they are visible.

4) The penalties associated with the installation of the IRSS system are restricted to a minimum in the conceptual design. The weight penalty is reduced by using lightweight composite and glass wool; both have low thermal conductivity, which reduces their thicknesses. The engine backpressure penalty is reduced by minimizing the disturbance to the exhaust flow and by avoiding excessive cooling of the exhaust gases within the flow path.

5) Because the engine exhaust flow is not disturbed, surfaces that are wetted by the flow are not completely blocked, but their visibility is restricted to a narrow range of ϕ.

Acknowledgments

The authors are grateful to the Rotary Wing Research and Design Centre, Hindustan Aeronautics Limited—Bangalore, for the financial support for this study. The authors thank the Centre for Aerospace Systems Design & Engineering (CASDE) of their department for the logistic support, and the A. von Humboldt Foundation, Germany, for the rich exposure to research methodology.

References

[1] Howe, D., "Introduction to the Basic Technology of Stealth Aircraft. 1. Basic Considerations and Aircraft Self-Emitted Signals (Passive Considerations)," *Journal of Engineering for Gas Turbines and Power*, Vol. 113, No. 1, 1991, pp. 75–79.

[2] Mahulikar, S. P., Sonawane, H. R., and Rao, G. A., "Infrared Signature Studies of Aerospace Vehicles," *Progress in Aerospace Sciences*, Vol. 43, Nos. 7–8, 2007, pp. 218–245. doi:10.1016/j.paerosci.2007.06.002

[3] May, J. J., Jr., and Vanzee, M. E., "Electrooptic and Infrared-Sensors," *Microwave Journal*, Vol. 26, No. 9, 1983, pp. 121–131.

[4] Gebbie, H. A., Harding, W. R., Hilsum, C., Pryce, A. W., and Roberts, V., "Atmospheric Transmission in the 1 to 14 μm Region," *Proceedings of the Royal Society of London Series A*, Vol. 206, No. 1084, 1951, pp. 87–107. doi:10.1098/rspa.1951.0058

[5] Jamieson, J. A., McFee, R. H., Plass, G. N., Grube, R. H., and Richards, R. G., *Infrared Physics and Engineering*, McGraw–Hill, New York, 1963, pp. 1–5.

[6] Varney, G. E., "Measuring Progress in IR Signature Technology," *Aerospace America*, Vol. 30, No. 8, 1992, p. 46.

[7] Sully, P. R., VanDam, D., Bird, J., and Luisi, D., "Development of a Tactical Helicopter Infrared Signature Suppression (IRSS) System," *Proceedings of the Flight Vehicle Integration Panel Symposium*, CP-592, AGARD, 1996.

[8] Thompson, J., Birk, A. M., and Cunningham, M., "Design of an Infrared Signature Suppressor for the Bell 205 (UH-1H) Helicopter. Part 1: Aerothermal Design," *Proceedings of 46th Annual Canadian Aeronautics and Space Institute (CASI) Conference*, May 1999.

[9] Blake, B. H. L., *Jane's Weapons Systems 1987–88*, Jane's Publishing, London, 1987.

[10] Lerner, E. J., "Tracking Missiles with Mosaic Starers," *Aerospace America*, Vol. 24, June 1986, pp. 52–55.

[11] Paterson, J., "Overview of Low Observable Technology and Its Effects on Combat Aircraft Survivability," *Journal of Aircraft*, Vol. 36, No. 2, 1999, pp. 380–388.

[12] Stead, A. J., and Missous, M., "Multicolour Infrared Detection with $In_{0.1}Ga_{0.9}As/Al_{0.33}Ga_{0.67}As$ Double and Triple-Coupled Quantum Well Infrared Photodetectors," *Proceedings of the Workshop on High Performance Electron Devices for Microwave and Optoelectronic Applications (EDMO)*, IEEE, Piscataway, NJ, 1999, pp. 119–124.

[13] Pruyn, R. R., and Windolph, W. G., "Survivability Tradeoff Considerations for Future Military Observation Helicopters," *Journal of the American Helicopter Society*, Vol. 24, No. 2, 1979.

[14] Mahulikar, S. P., Rao, G. A., Sane, S. K., and Marathe, A. G., "Aircraft Plume Infrared Signature in Nonafterburning Mode," *Journal of Thermophysics and Heat Transfer*, Vol. 19, No. 3, 2005, pp. 413–415.

[15] Rao, G. A., and Mahulikar, S. P., "Effect of Atmospheric Transmission and Radiance on Aircraft Infrared Signatures," *Journal of Aircraft*, Vol. 42, No. 4, 2005, pp. 1046–1054.

[16] Mahulikar, S. P., Rao, G. A., and Kolhe, P. S., Infrared Signatures of Low Flying Aircraft and Their Rear Fuselage Skin's Emissivity Optimization, *Journal of Aircraft*, Vol. 43, No. 1, 2006, pp. 226–232.

[17] Mahulikar, S. P., Sane, S. K., Gaitonde, U. N., and Marathe A. G., "Numerical Studies of Infrared Signature Levels of Complete Aircraft," *The Aeronautical Journal*, Vol. 105, No. 1046, 2001, pp. 185–192.

[18] Mahulikar, S. P., Kolhe, P. S., and Rao, G. A., "Skin Temperature Prediction of Aircraft Rear Fuselage with Multi-Mode Thermal

Model," *Journal of Thermophysics and Heat Transfer*, Vol. 19, No. 1, 2005, pp. 114–124.

[19] Hudson, R. D., Jr., *Infrared System Engineering*, Wiley, New York, 1969, p. 35.

[20] Rao, G. A., and Mahulikar, S. P., "New Criterion for Aircraft Susceptibility to Infrared Homing Missiles," *Aerospace Science and Technology*, Vol. 9, No. 8, 2005, pp. 701–712. doi:10.1016/j.ast.2005.07.005

[21] Mahulikar, S. P., Potnuru, S. K., and Kolhe, P. S., "Analytical Estimation of Solid Angle Subtended by Complex Well Resolved Surfaces for Infrared Detection Studies," *Applied Optics*, Vol. 46, No. 24, 2007, pp. 4991–4998.

C. Tan
Associate Editor